

# Divalent Metal Complexes Of Azosulfamethaxazole: Synthesis And Characterization With Study Some Of Their Applications

Duaa Jameel Jasim , Alyaakhider Abbas

Department of Chemistry, College of Science, University of Baghdad, Baghdad

<sup>1</sup>duaajameel321@gmail.com

<sup>2</sup>[aalyaakhider@yahoo.com](mailto:aalyaakhider@yahoo.com)

---

## Abstract

By diazotization and coupling for theobromine and sulfamethoxazole, the novel [4-(8-theobromine azo) sulfamethoxazole] (TAS) has been produced. To make new complexes, the ligand (TAS) was reacted with [Pd (II), Pt (II), and Co(II)]. Spectroscopic methods, thermal analysis, molar conductance data, and magnetic measurements were utilized to analyze both the (TAS) ligand and its metal complexes. The technique of mole ratio was used to determine the stoichiometric of the complexes, which was [1:2] [M:L] except Pd(TAS) it found [1:1]. The complexes of Pt(II) and Pd(II) exhibited square planar geometry, whereas Co(II) was determined to be octahedral geometry. For the TAS ligand and its complexes, the dyeing performance and antibacterial properties were studied. The Palladium complex was also investigated as an antioxidant.

**Keywords:** sulfamethoxazole, antioxidant, antibacterial, dyeing performance, complexes

---

## Introduction

Azo dyes can be considered as the most fundamental type of organic compounds are widely used in a variety of sectors because of their versatility and highly colored complexes [1] they had popularly utilized as a pigment, dyes cosmetics, food coloring, toys and are well recognized for biological activity such as antibacterial, antifungal and anti-inflammatory [2]. Sulfamethoxazole (SMX) is a kind of sulfonamide. bacteriostatic antibiotic. The sulfonamides activity in the biological aspect has gained much attention and is well documented. Its uses are very wide and in many different applications such as their use as antibacterial and antitumor agents. In the past decade, the treatment of numerous ailments using metal-based therapeutics has received great interest. Biologically, the compounds of sulfonamide are active molecules [3]. Theobromine (TBR) is a popular alkaloid that can be found in structures of coffee,

tea, cacao, etc. It has familiar pharmacological and biological activities for the living organisms[4]. Theobromine, caffeine, and theophylline, methyl-substituted xanthines, are key ingredients in a wide range of drinks (cocoa, tea, coffee, and chocolate products), as well as therapeutic. There is continuing interest and investigation in their pharmacological properties and due to their capability of sensitizing alkylating compounds to protect cells from the harmful effects of UV light, they have relevance to cancer therapy [5]. In the present paper, we report the synthesis of a new diazo ligand (TAS) has the IUPAC name [4-(8-theobromine azo) sulfamethoxazole] and its complexes with the metal ions [Pd (II), Pt (II), and Co(II)]. The spectral behaviors and physicochemical properties were investigated. The antioxidant and antimicrobial activities as well as the dyeing performance for wool were investigated.

## Experimental

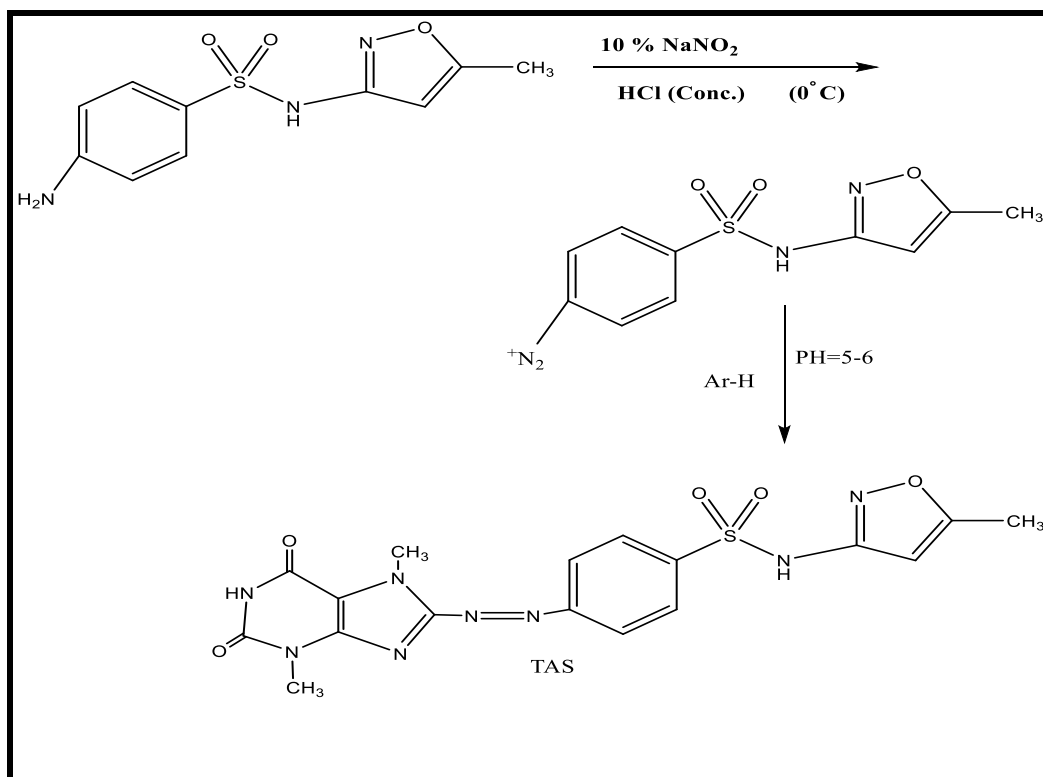
### Instruments and Materials

The materials and solvents were used of the highest possible grade. Metal content and elemental analysis for the (TAS) ligand and its metal complexes were obtained using (C.H.N.S), and the proportion of metal in complexes was calculated using (Eure EA 3000 Elemental analyzer). FT-IR spectrophotometry was performed using a "Nova 350 spectrophotometer" Flam Atomic Absorption Spectrophotometer. UV-Vis Spectra for all the investigated compounds were recorded on the (SHIMADZU 1800- UV spectrophotometer) using ethanol in the range of (200-1100) nm using the SHIMADZU 8400s spectrophotometer in the region of (250- 4000)  $\text{cm}^{-1}$  with CsI. The  $^1\text{H}$ NMR spectra were obtained with tetramethylsilane as the internal standard on a BRUKER AV 400 Advance -III (400 MHz and 100 MHz) equipment. The metal content of the produced ligands and complexes was evaluated by thermal analysis (TG) (SDT Q600 V20.9 Build). Stuart melting point equipment was used to determine the melting points of all the compounds. In ethanol ( $10^{-3}$  M), the molar conductance of metal ion complexes was investigated using HI 9811-5" HANNA equipment. The Mohr technique was utilized to determine the chloride content of the materials examined. M.S.B. is the model's name. At room temperature, the magnetic susceptibility of the investigated complexes was evaluated utilizing the Auto Apparatus.

### 1-Synthesis of (TAS) ligand

As mentioned in the literature [6] with some modification, the synthesis was done for the ligand [4-(8-theobromine azo) sulfamethoxazole] (TAS). The diazonium salt was synthesized by dissolving (2.53 gm; 0.01 mole) sulfamethoxazole in (10 ml) distilled water and then adding (10 ml) concentrated HCl, then cooled 10%  $\text{NaNO}_2$  solution was added to the mixture which had been chilled in an ice bath ( $0^\circ\text{C}$ ), with

stirring for (1hour). the solution of diazonium salt was slowly added to an alcoholic alkaline solution of theobromine (1.8;gm 0.01 mole). After that, the solution's pH was adjusted to (5-6). Leave it overnight to precipitate. The colored powder that resulted was filtered and dried after washing it by ethanol: water [1:1] and dry. scheme (1)



**Scheme (1):synthesis of TAS ligand**

## 2-Metal complex synthesis

The ligand(TAS)in an ethanolic solution [0.89gm,0.001M] is added to each of the ethanolic solution of the chloride salt for selected metals [Co (II) , Pd(II) and Pt (II)] (0.001M) (0. 237, 0.177, and 0.41) gm respectively in terms of mole ratio [1:2] [M:L]. The combination then was refluxed for three hours, and the results were analyzed using a TLC technique. The color precipitate is filtered and rinsed with ethanol many times. It was then allowed to dry. Table (1) appeared properties of the synthesized compounds

**Table (1): Some data from analytic and physical sources for the TAS ligand and its complexes**

	M:L	Color $\lambda$ (nm)	% Experimental % (Theoretical)	( $\Delta m$ ) oh

Comp. (M.wt) (gm/mol)			C	H	N	S	M	Cl	$m^{-1} cm^2 mol^{-1}$
TAS(C <sub>17</sub> H <sub>17</sub> N <sub>8</sub> O <sub>5</sub> S) (445.44)	-	Pale Yellow (362)	45.35 45.79	3.92 3.81	24.51 25.14	7.93 7.18	-	-	-
Pt(C <sub>17</sub> H <sub>17</sub> N <sub>8</sub> O <sub>5</sub> S) <sub>2</sub> Cl <sub>2</sub> .2H <sub>2</sub> O (1192.88)	1:2	Green-brown (610)	33.67 34.20	4.09 3.18	19.24 18.77	5.12 5.36	16.8 4 16.3 4	5.66 5.95	85
Pd(C <sub>17</sub> H <sub>17</sub> N <sub>8</sub> O <sub>5</sub> S)Cl <sub>2</sub> (622.86)	1:1	red brown (505)	33.07 32.75	2.35 2.72	18.46 17.98	4.83 5.13	17.4 3 17.0 8	11.8 6 11.3 9	8.25
Co(C <sub>17</sub> H <sub>17</sub> N <sub>8</sub> O <sub>5</sub> S) <sub>2</sub> Cl <sub>2</sub> (1020.78)	1:2	Pink (536)	40.33 39.96	3.91 3.33	22.46 21.94	6.52 6.26	5.23 5.77	7.12 6.95	18

### 3-Anti-oxidant and Radical Scavenging Activity

To test the reductive ability, 1 ml of each concentration of [Pd(TAS)Cl<sub>2</sub>] (0.08, 0.16, 0.32, and 0.64 mg/ml). After mixing with 1 ml of 0.2M phosphate buffer (pH 6.6) and 1.5 ml of 1 percent potassium ferricyanide, the mixture was incubated at 50°C for 20 minutes, as reported in the literature [7]. 1 ml of 10% trichloroacetic acid was added to the liquid to stop the reaction. 2.5 ml of the supernatant, 2 ml distilled water, and 0.5 ml of freshly made 1 percent ferric chloride were mixed after centrifugation for 10 minutes at 3000 pm. After that, at 700nm, the absorbance was measured. The trolox solutions were treated in the same way (standards). All of the tests were carried out in duplicate. Based on the stable DPPH free radical's radical scavenging activity, the antioxidant activity of the [Pd(TAS)Cl<sub>2</sub>] and standard (vitamin C) were evaluated using the technique of [8]. In a test tube, 3.9 ml of DPPH solution was mixed

with an aliquot of 0.1 ml of each of the two complexes or standard (0.625, 0.125, 0.250, and 0.500 mg/ml). A spectrophotometer was used to determine the absorbance of each solution at 517nm after 30 minutes of incubation at 37°C. Triplicates of all measurements were taken. The following equation was used to calculate the ability to scavenge DPPH radicals:

$$\text{DPPH radical scavenging activity (\%)} = \left( 1 - \frac{\text{Absorbance of Sample}}{\text{Absorbance of Standard}} \right) \times 100$$

#### **4-Antibacterial and antifungal of synthesized ligand and its complexes**

The efficacy of antibacterial of the new azo ligand (TAS) and its complexes was tested in vitro with two pathogenic microorganisms using a disk diffusion technique in (10<sup>-3</sup>M) ethanol as a solvent [9], Inhibitory zones (in mm) were measured after the Petri dishes were incubated for 24 hours at 37°C (for bacteria) and 72 hours (for fungi), with sulfamethoxazole as a control for bacteria and fluconazole for fungi. The pathogenic microorganisms utilized were chosen because they may cause a wide spectrum of life-threatening disorders in living systems. There were gram-positive bacteria *Staphylococcus aureus* (Staph) and gram-negative bacteria *Escherichia Coli*(E.coli) while the one type of fungi (*Rhizopusmicrosporus*).

#### **5-Dying Method**

In the wool fabric, the coloring characteristics of the ligand (TAS) and its complexes were used. (0.3 gm) of azo dyes (TAS) ligand and its complexes were dissolved in an ethanolic solution of 10% NaOH, then added 50ml of distilled water. After that, A piece of clean white wool fabric(10×10) cm, (30gm ± 3gm) that soaked in distilled water for (30) minutes was transferred to the azo dye solution and heated to (60) °C for (10) minutes. The soaked cotton fabric piece was washed three times with (250) ml distilled water containing (1 gm) of soap to remove any non-reacting species. Finally, dyed raw was dried by hot steam [10]

### **Results and Discussion**

#### **1-The mole ratio**

The mole ratio approach was used to evaluate the stoichiometric reaction of the ligand (TAS) and its [Pd (II), Pt (II), and Co(II)] complexes. This is the most well-known approach for determining the type of complexes generated in the solution that requires separation when the amount of ligand is altered

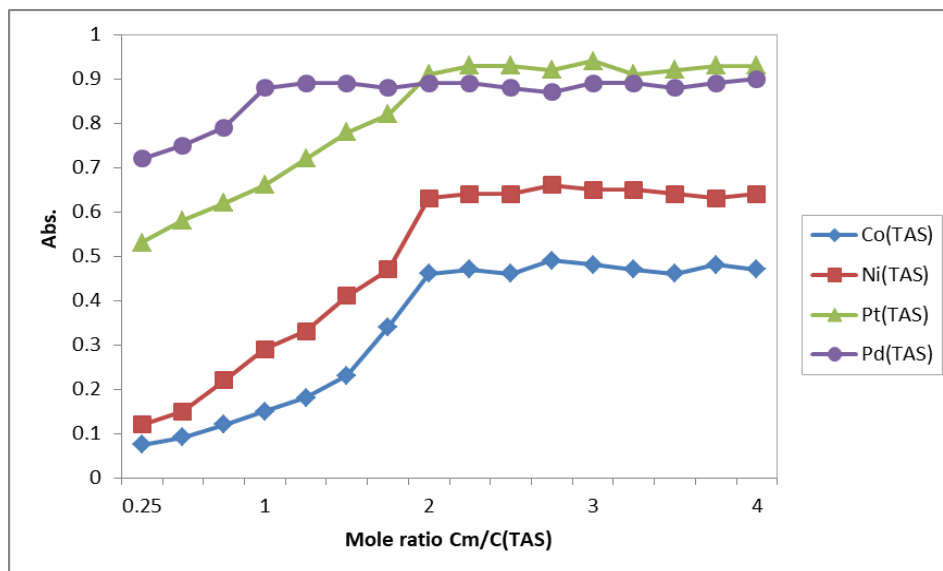
(0.25ml) and the amount of metal ion is kept constant, this technique was utilized to test the absorbance vs molar ratio of the (M:L).[10]

The relationship between the (M:L) ratio and the absorbance is shown in Figure (1), while the results are collected in Table (2). The Co(II) and Pt(II) have a (1:2) (M:L) ratio, while the Pd(II) complex has (1:1)(M:L) ratio

**Table (2): TAS-Metal ion solution absorbance vs mole ratio**

M:L	Absorbance		
	Co(TAS)	Pt(TAS)	Pd(TAS)
1:0.25	0.075	0.53	0.72
1:0.50	0.091	0.58	0.75
1:0.75	0.12	0.62	0.79
1:1	0.15	0.66	0.88
1:1.25	0.18	0.72	0.89
1:1.50	0.23	0.78	0.89
1:1.75	0.34	0.82	0.88
1:2	0.46	0.91	0.89
1:2.25	0.47	0.93	0.88
1:2.50	0.46	0.93	0.87
1:2.75	0.49	0.92	0.89
1:3	0.48	0.94	0.89
1:3.25	0.47	0.91	0.88
1:3.50	0.46	0.92	0.89
1:3.75	0.48	0.93	0.90
1:4	0.47	0.93	0.89

**Figure (1): the mole ratio of (TAS) ligand and its complexes**



## 2-Gibbs free energy and stability constant

The stability constant can be calculated spectrophotometrically [11]. For complexes with a mole ratio of [M: L] [1:2] was calculated using the equations below.

$$K = \frac{(1 - \alpha)}{4\alpha^3 c^2} \qquad \alpha = \frac{(A_m - A_s)}{A_m}$$

C= (molar concentration) for the complexes in molar (c = 10<sup>-3</sup>M)

α = degree of disintegration

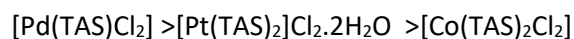
A<sub>m</sub> = the solution's absorption which contains (volume of the metal and additional ligand)

A<sub>s</sub> = solution absorption that consists (1:1) stoichiometric (M:L)

Except for [Pd(II)-TAS] (1:1) (M:L), where the following equation was used to calculate the mole ratio, the preceding formulae can be used to all produced complexes.

$$K = \frac{(1 - \alpha)}{\alpha^2 c}$$

The results were shown in the table (3), so the stability increases in the following order :



The thermodynamic coefficients of ΔG (Gibbs free energy) were obtained from the below equation [12]:

$$\Delta G = - RT \ln K$$

Where:

R= constant of the gas that equals 8.31 J. mole<sup>-1</sup>. K

T = absolute temperature (Kelvin)

The formations we got through  $\Delta G$  that the synthesis of all complexes is spontaneous.

Table (3) shows the behavior of the thermodynamic parameters of  $\Delta G$  (Gibbs free energy):

**Table (3): The Gibbs free energy ( $\Delta G$ ) and the stability constant (K) for the synthesized complexes.**

Complex	As	Am	K	Ln K	$\Delta G$ (J/mole)
[Co(TAS) <sub>2</sub> Cl <sub>2</sub> ]	0.15	0.46	275000	12.52	-32004.27
[Pt(TAS) <sub>2</sub> ]Cl <sub>2</sub> .2H <sub>2</sub> O	0.66	0.91	875966.18	13.68	-33876.87
[Pd(TAS)Cl <sub>2</sub> ]	0.88	0.89	7840355.74	15.87	-39300.15

### 3-The FT-IR spectra

Table (4) was contained the principal FT-IRvibration bands of the (TAS) ligand and its complexes,which diagnostic to the mode of coordination of the ligand (TAS), While their spectra were taken in the region(400-4000)cm<sup>-1</sup>[Figures (2)-(5)]show the spectra.

- 1) The band for the azo moiety in the free ligand at(1485,1460) cm<sup>-1</sup>was shifted to a lower wavelength in the range  $\nu$  (1461,1441)- (1473,1445) cm<sup>-1</sup> after complexation, showing that the azonitrogen atoms are in a state of coordination with the metal ion [13]. So this band was shifted when was compared between the spectra of the complexes to that of a free ligand (TAS).As well as having another band corresponding to the azo stretching modes  $\nu$  (C-N=N-C)which was noticed in a spectrum of the free ligand and appeared many changes in the shape and region by complexation [10] [Table (4)].
- 2) The bands  $\nu$  (N-H),  $\nu$  (C=O) and  $\nu$  (SO<sub>2</sub>) in the FT-IR spectrum for the free ligand (TAS) were unaffected in the complexes spectra, implying that there was no chelating via these moieties ,but the little changes were appeared in the position or shape sometimes attributed to decrease or increase or resonance due to chelating[14,15]



- 3) The ligand (TAS) was demonstrated a doublet band at (1550,1596)  $\text{cm}^{-1}$  which referred to the imine moiety  $\nu(\text{C}=\text{N})$  for isoxazole ring in sulfamethoxazole and imidazole ring in theobromine respectively. Slight changes occurred in these bands in the spectrum for the complexes when compared with the ligand spectrum, despite the interaction between the metal ion and the ligand (TAS) at the nitrogen atom of the  $\nu(\text{C}=\text{N})_{\text{imd}}$ , due to the overlap of these bands with  $\nu(\text{C}=\text{N})_{\text{iso}}$ [15].
- 4) Due to the creation of  $\nu(\text{M}-\text{N})_{\text{azo}}$  and  $\nu(\text{M}-\text{Cl})$  bonds, the spectra of all the complexes reveal new bands in the area (434-459)  $\text{cm}^{-1}$  and (308-312)  $\text{cm}^{-1}$ , respectively[16,17]. As well as the emergence of additional bands at (613-615)  $\text{cm}^{-1}$  that were attributed to  $(\text{M}-\text{N})_{\text{imd}}$ , When comparing metal complexes' spectra to the spectra of the free ligand(TAS)[10].
- 5) We conclude for the above that the ligand (TAS) acts as neutral N,N-bidentat through nitrogen atom for azo moiety and nitrogen atom for imine moiety in theobromine.

**Table (4): FTIR spectra data for the (TAS) ligand and its complexes**

Assessment center	$\nu(\text{OH})_{\text{H}_2\text{O}}$ $\nu(\text{OH})_{\text{phenolic}}$	$\nu(\text{N}-\text{H})$	$\nu(\text{C}=\text{N})_{\text{iso}}$ $\nu(\text{C}=\text{C})_{\text{imd}}$	$\nu(\text{C}=\text{O})$	$\nu(\text{N}=\text{N})$	$\nu(\text{C}-\text{N}=\text{N}-\text{C})$	$\nu(\text{SO}_2)$	$\nu(\text{M}-\text{N})_{\text{imd}}$	$\nu(\text{M}-\text{N})_{\text{azo}}$	$\nu(\text{M}-\text{Cl})$
TAS	- -	3114 T.w. 3159 T.w. 3178 T.w.	1550 v w 1596 w	1691 S	1485 w 1460 w	1396 w.	1332 w 1292 w	-	-	-
Co (II)	- -	3114 w 3161 w	1548 m. 1595 m	1691 S.	1461 m 1441 m	1365 m	1334 w. 1285 m	615 m	434 m.	308 S
Pd(II)	- -	3114 w 3166 w	1550 m 1595 m	1693 1673 d S.	1462 m 1438 m	1367 w.	1334 w 1294 w	615 m	455 m	312 m.
Pt(II)	3433 br.m	3112w 3176w	1554 w 1591 v.w.	1691 s 1668 m	1473 w 1445 w	1373 w	1338 w 1296 w	613 w	459 w	-

w:weak s:strong m:medium d:double t:triple iso: isoxazoleim d: imidazole br: broad

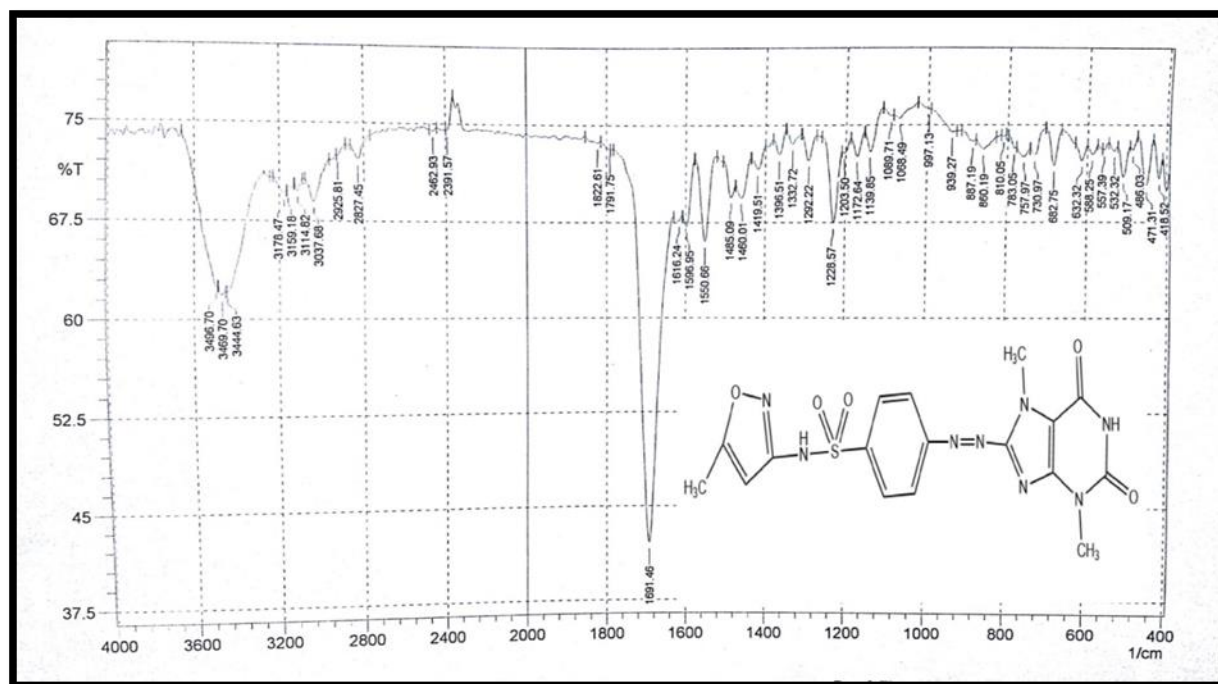


Figure (2): FTIR spectrum of (TAS) ligand

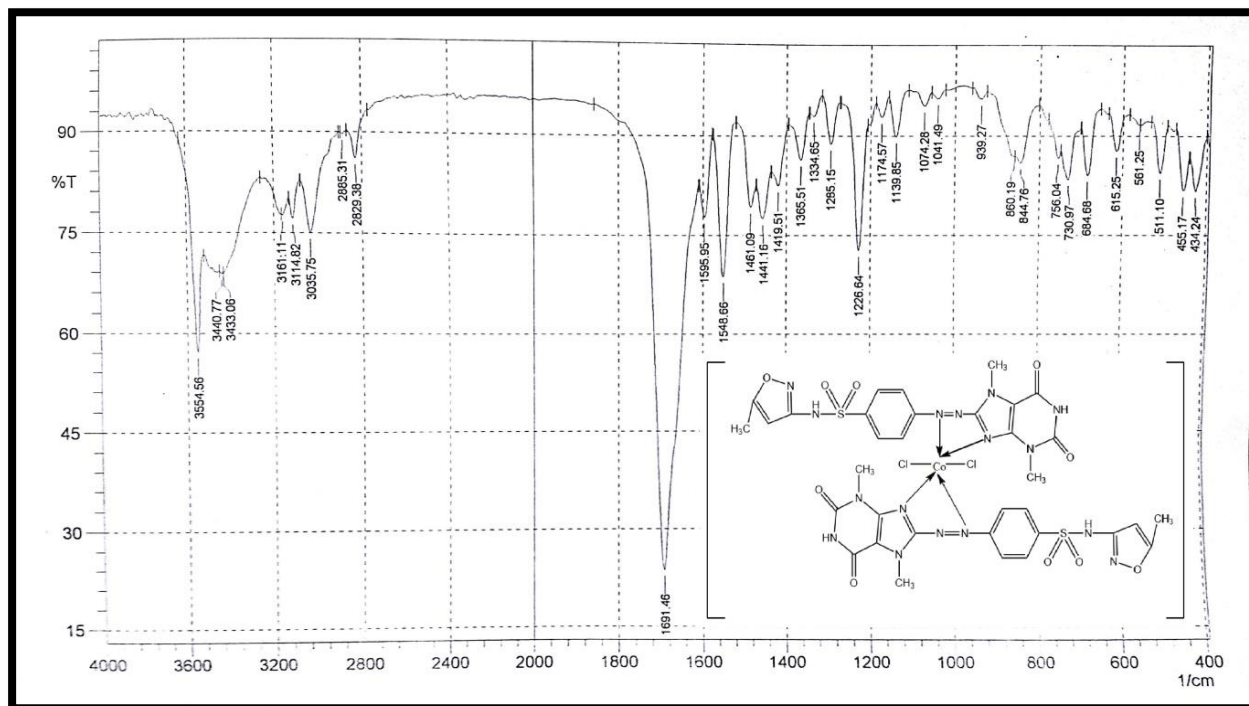


Figure (3): FTIR spectrum of  $[Co(TAS)_2Cl_2]$  complex

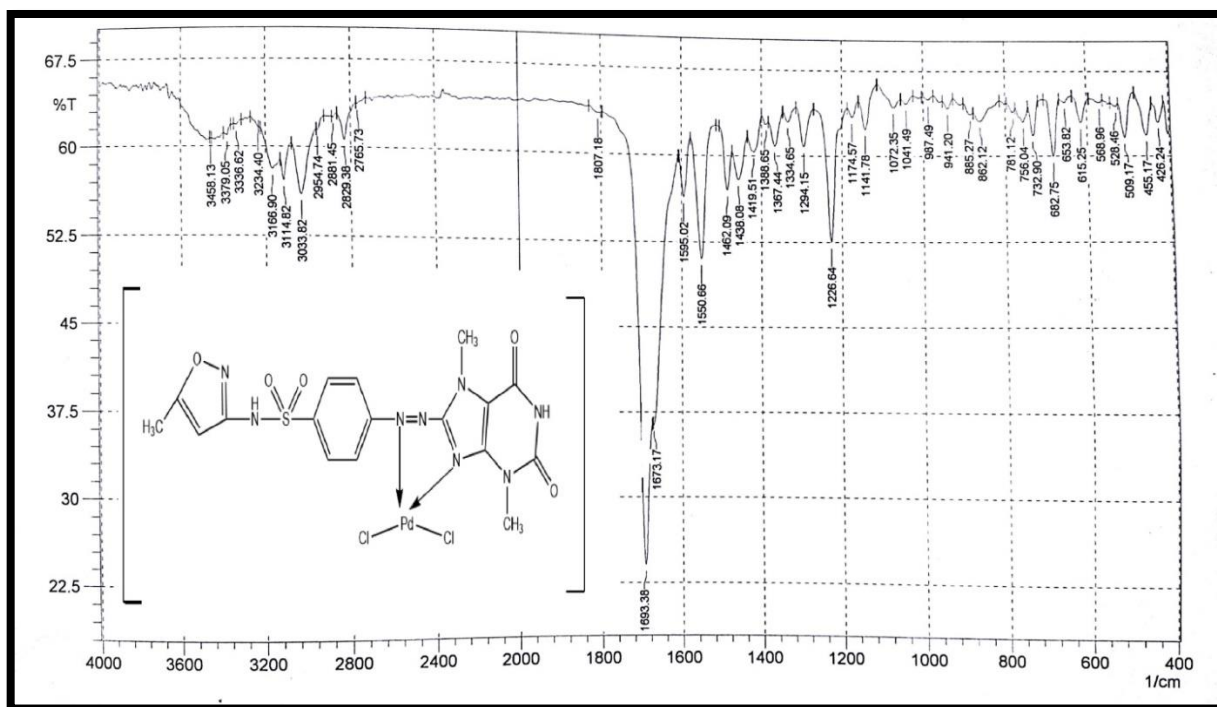


Figure (4): FTIR spectrum of  $[Pd(TAS)Cl_2]$  complex

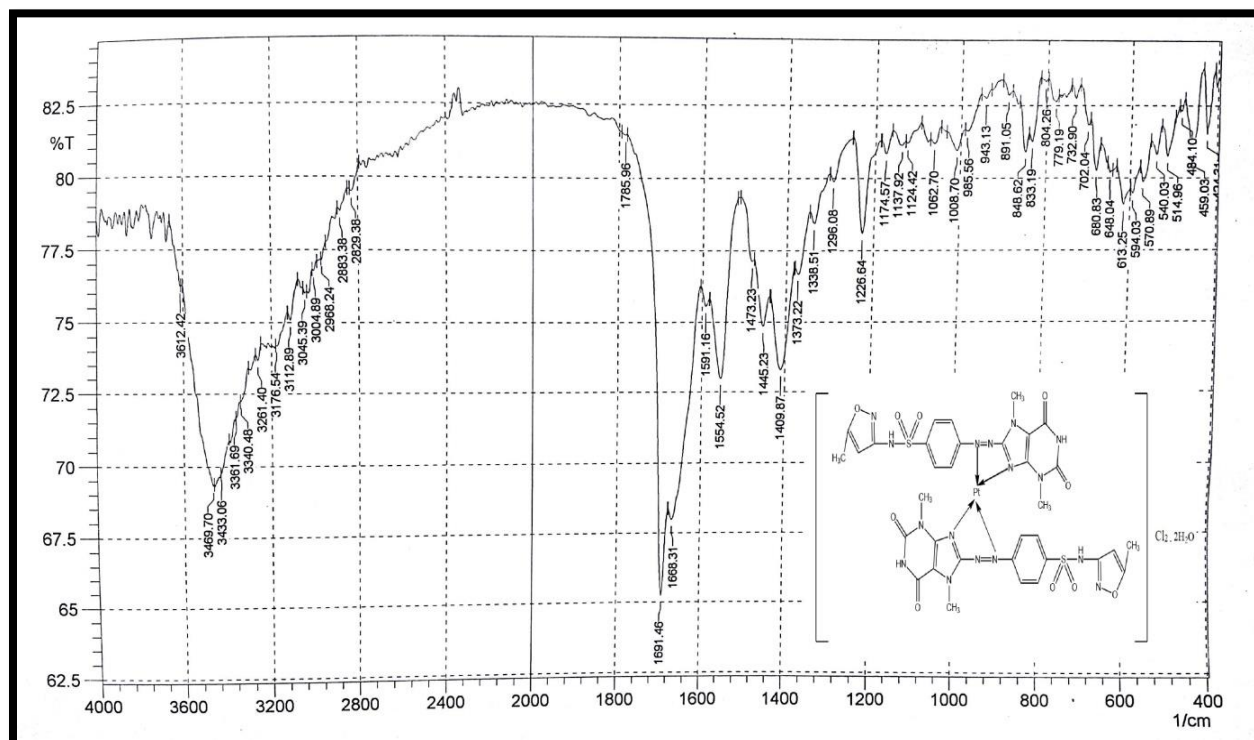


Figure (5): FTIR spectrum of  $[Pt(TAS)_2]Cl_2 \cdot 2H_2O$  complex

#### 4- $^1H$ -NMR spectra

The results obtained from the FTIR spectra are further supported by the  $^1H$ -NMR analyses. It is accomplished by comparing the changes in the  $^1H$ NMR spectra of generated complexes to those of free ligand. Table (5) shows the data for the shifting ( $\delta$ ) in ppm for several kinds of protons in the ligand (TAS) and its complexes for Pt(II) and Pd(II), while the  $^1H$ NMR spectra were obtained in DMSO- $d_6$  solution [Figures (6-8)].

The free ligand (TAS) shows signals in a field at (11.12)ppm,(2.53)ppm and the multiplet signals observed in the range [(7.99-8.13)ppm for NH-sulfa ,CH<sub>3</sub>-oxazol, and Ar-Hbenzen respectively [1]. The free ligand (TAS)shows signals at(11.00, 3.86, and 3.35) ppm for NH-pyrm, N-CH<sub>3</sub>imd, and N-CH<sub>3</sub>pyrm respectively[18]. In the spectra of Pt(II) and Pd(II)complexes, The signals were a light shift that refers to non-sharing of these groups in coordination with metal ions.

Table (5):  $^1H$ NMR signals of TAS ligand and its complexes

Comp.	NH <sub>sulfa</sub>	Ar-	CH <sub>3</sub> oxazol	CH <sub>oxazol</sub>	N-CH <sub>3</sub> imd	N-CH <sub>3</sub> pyrm	H <sub>2</sub> O
-------	---------------------	-----	------------------------	----------------------	-----------------------	------------------------	------------------

	NH <sub>pyrm</sub>	H <sub>benzen</sub>					
TAS	11.12 11.00	7.99- 8.13	2.53	6.13	3.86	3.35	-
[Pd(TAS) Cl <sub>2</sub> ]	11.13 11.00	7.97- 8.00	2.52	6.13	3.87	3.35	-
[Pt(TAS) <sub>2</sub> ]Cl <sub>2</sub> ·2H <sub>2</sub> O	11.14 11.06	7.97- 7.82	2.52	6.25	3.87	3.35	3.41

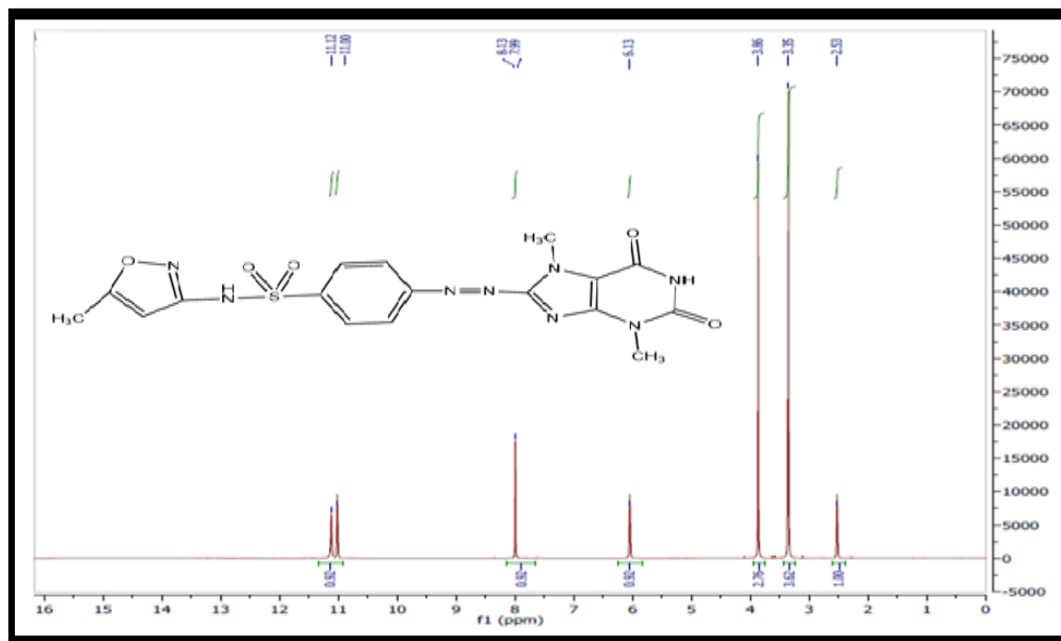


Figure (6):  $^1\text{H}$ NMR Spectrum for the TAS ligand

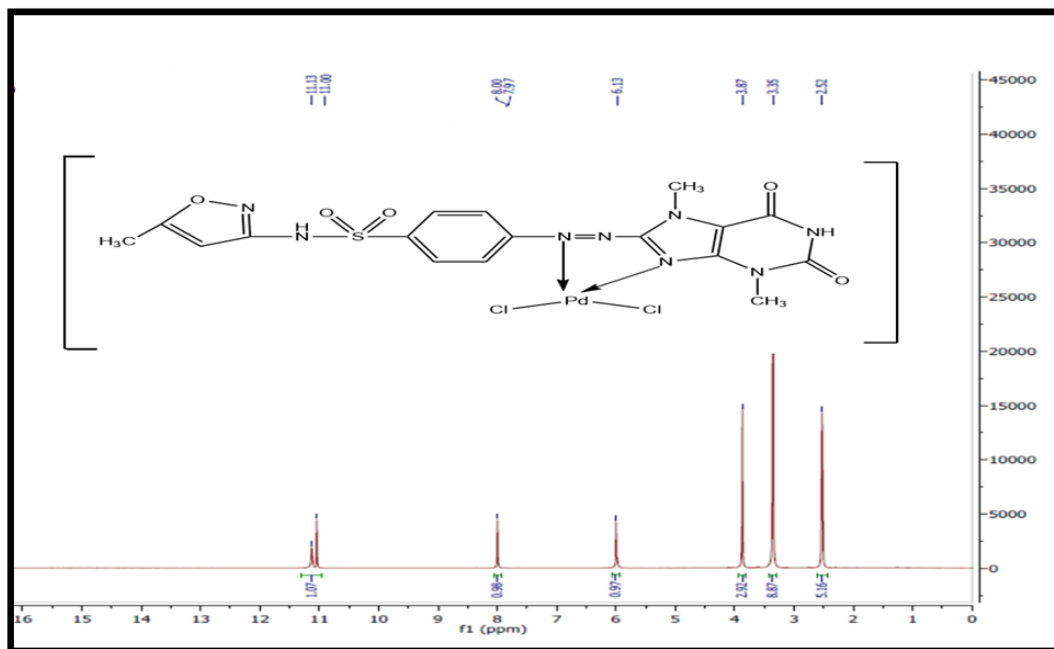


Figure (7):  $^1\text{H}$ NMR Spectrum for the  $[\text{Pd}(\text{TAS})\text{Cl}_2]$  complex

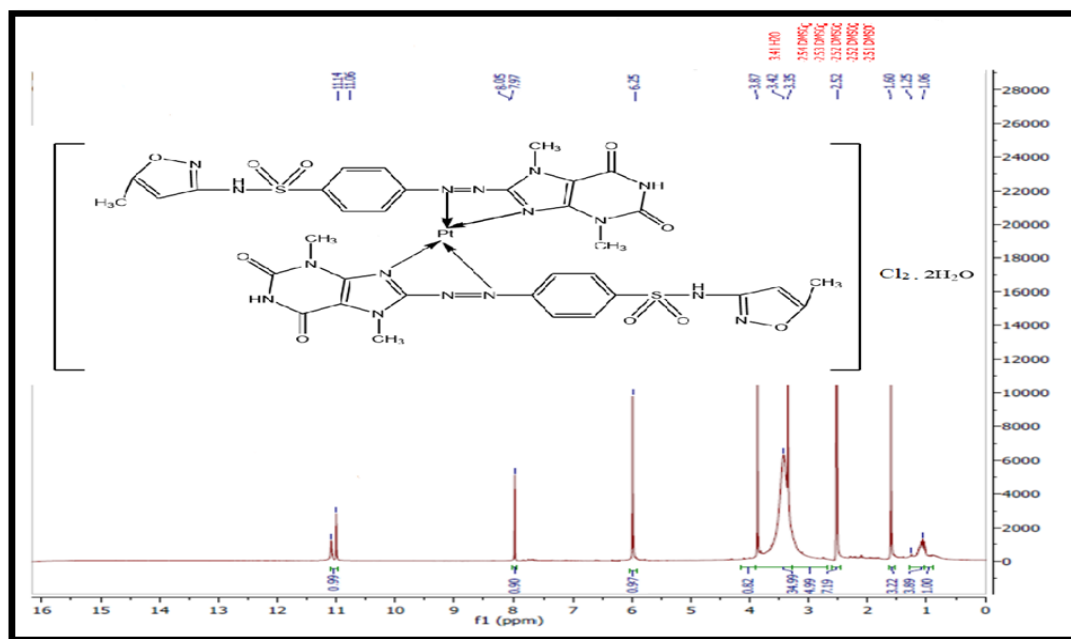


Figure (8):  $^1\text{H}$ NMR Spectrum for the  $[\text{Pt}(\text{TAS})_2]\text{Cl}_2 \cdot 2\text{H}_2\text{O}$  complex

## 5-Electronic-spectrum and magnetic properties

The geometry of solid complexes can be determined by looking at their electronic spectra. As a result, electronic spectrum features were concentrated on the discrepancies between the molecule's ground and excited states [19]. Table (6) lists the results of the electronic absorption for the ligand (TAS) and its complexes within ( $10^{-4}$ ) molar in ethanol at room temperature, whereas Figures [(9)-(12)] explain their spectra. The synthesized compounds' electronic spectra revealed novel bands. The locations and intensities of the bands are primarily determined by relying on the ligand field effect, metal ion-electron configuration, and complex stereochemistry [20].

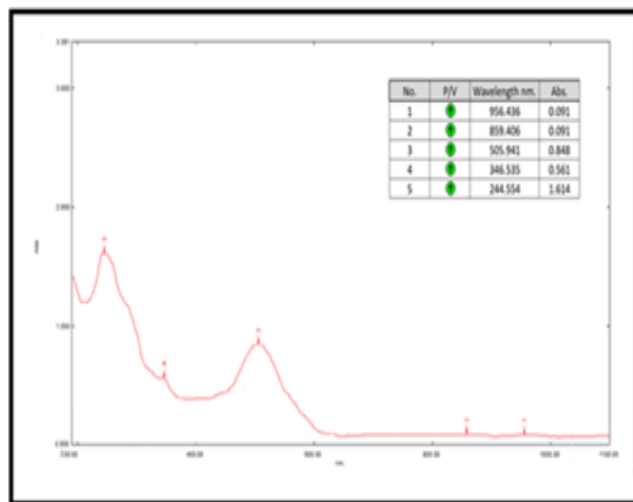
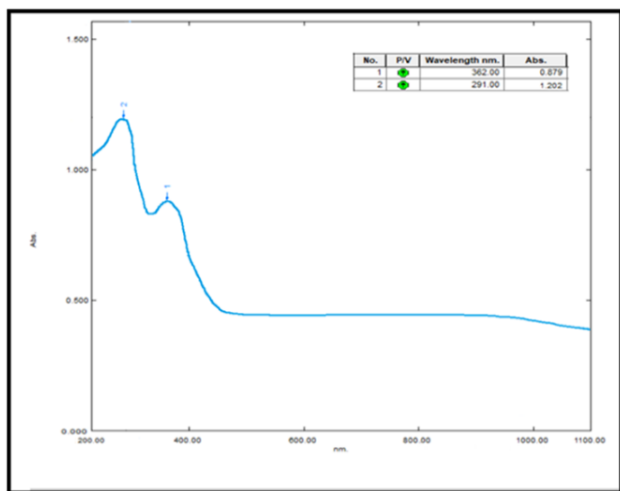
The UV-Vis spectrum of the ligand (TAS) in ethanol with the extent (200-1100) nm, [Figure(9)] displays mainly two peaks. The first peak at (291nm,  $34364\text{ cm}^{-1}$ ), for (TAS) which was attributed to benzene mild energy ( $\pi \rightarrow \pi^*$ ) transition for pyrimidine and aromatic moieties. The second peak at (362 nm,  $27624$ ) was related to the ( $n \rightarrow \pi^*$ ) transition of intramolecular charge transfer taking place via the azo moiety [20].

In the spectra of the low spin ( $d^8$ ) Pd (II) complex [Figure (10)], with square planar geometry, three (d-d) transitions were anticipated. ( $d^8$ ) $^1A_{1g} \rightarrow ^1A_{2g}$ ,  $^1A_{1g} \rightarrow ^1B_{1g}$  and  $^1A_{1g} \rightarrow ^1E_{1g}$  [10]. Only two transitions were observed at (956nm;  $10460\text{ cm}^{-1}$  and 859nm;  $11641\text{ cm}^{-1}$ ) for [Pd (TAS)Cl<sub>2</sub>] which belong to  $^1A_{1g} \rightarrow ^1A_{2g}$  and  $^1A_{1g} \rightarrow ^1E_{1g}$ . While the transitions  $^1A_{1g} \rightarrow ^1B_{1g}$  it is too weak to appear. But regarding the peak at (505nm;  $19801\text{ cm}^{-1}$ ) for [Pd(TAS)Cl<sub>2</sub>] was attributed to LMCT[21].

In the spectrum of the [Co(TAS)<sub>2</sub>Cl<sub>2</sub>] complex [Figure (11)], It has three electronic transitions: the first at (899nm;  $11123\text{ cm}^{-1}$ ) belong to the  $^4T_{1g(F)} \rightarrow ^4T_{2g(F)}$ , the second at (751nm;  $13315\text{ cm}^{-1}$ )  $^4T_{1g(F)} \rightarrow ^4A_{2g(F)}$ , the third transition peak ( $^4T_{1g(F)} \rightarrow ^4T_{1g(P)}$ ) may be obscured by the complex peak at (536nm;  $18656\text{ cm}^{-1}$ ). The complex has octahedral geometry[22].

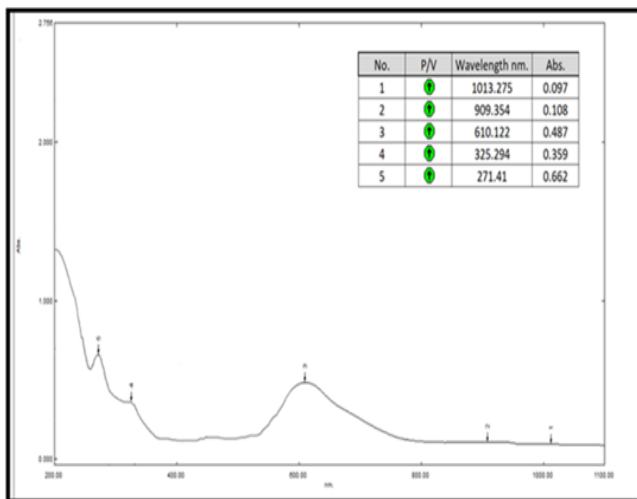
The value of the magnetic measurement for low spin  $d^8$ Pt(II)- complex is zero, which is approaching the value of the four-coordinate square planar geometry [23,24]. Two (d-d) transitions were shown in Figure (12) as explained below for [Pt (TAS)<sub>2</sub>]Cl<sub>2</sub>.2H<sub>2</sub>O.

[ $^1A_{1g} \rightarrow ^1B_{1g}$  (909 nm;  $11001 \text{ cm}^{-1}$ ) and  $^1A_{1g} \rightarrow ^1A_{2g}$  (1013nm;  $9871 \text{ cm}^{-1}$ )]. The peak at (610 nm; 16393



$\text{cm}^{-1}$ ) was related LMCT.

Fig.(9): The spectrum of UV-Vis for the TAS ligand Fig. (10):The spectrum of UV-Vis for the



[Pd(TAS)Cl<sub>2</sub>]Complex

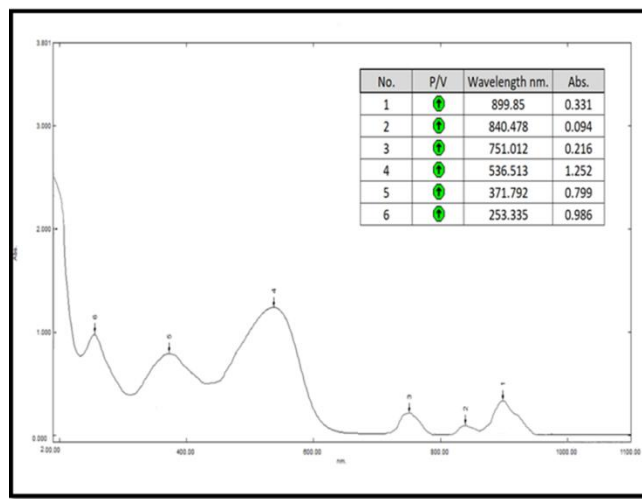


Fig. (12): The spectrum of UV-Vis for the [Pt(TAS)<sub>2</sub>]Cl<sub>2</sub>. 2H<sub>2</sub>O Complex Fig. (11): The Spectrum of UV-Vis for the [Co(TAS)<sub>2</sub>]Cl<sub>2</sub>Complex.



**Table (6): The ligand (TAS) and its complexes' electronic transition, hybridization, and geometry at (10<sup>-4</sup>M)**

Compound	$\lambda(nm)$	Wavenumber ( $cm^{-1}$ )	Assignment	hybridization	Geometry
TAS	362	27624	$n \rightarrow \pi^*$	-	-
	291	34364	$\pi \rightarrow \pi^*$		
[Co(TAS) <sub>2</sub> Cl <sub>2</sub> ]	899	11123	$^4T_{1g(F)} \rightarrow ^4T_{2g(F)}$	$sp^3d^2$	octahedral
	751	13315	$^4T_{1g(F)} \rightarrow ^4A_{2g(F)}$		
	536	18656	LMCT		
	371	26954	$n \rightarrow \pi^*$		
	253	39525	$\pi \rightarrow \pi^*$		
[Pd(TAS)Cl <sub>2</sub> ]	956	10460	$^1A_{1g} \rightarrow ^1A_{2g}$	$dsp^2$	Square planer
	859	11641	$^1A_{1g} \rightarrow ^1E_{1g}$		
	505	19801	LMCT		
	346	28901	$n \rightarrow \pi^*$		
	244	40983	$\pi \rightarrow \pi^*$		
[Pt(TAS) <sub>2</sub> ]Cl <sub>2</sub> .2H <sub>2</sub> O	1013	9871	$^1A_{1g} \rightarrow ^1B_{1g}$	$dsp^2$	Square planer
	909	11001	$^1A_{1g} \rightarrow ^1A_{2g}$		
	610	16393	LMCT		
	325	30769	$\pi \rightarrow \pi^*$		
	271	36900	$\pi \rightarrow \pi^*$		

### 6-Thermogravimetric Analysis (TGA)

The thermal behavior of the synthesized ligand (TAS) and complexes of the ligand was investigated by thermograms (TGA) as wereshown in Figures [(13)-(16)], while the changing number of the stage; mass losses were estimated and discovered are listed in Table (7). In our research, the weight loss followed up in the temperature range (25-1000) °C and was subjected to argon flow. The main goal of thermal analysis is to obtain information about stoichiometry, thermal stability, and if there is water molecules are crystallized or coordinated. The weight losses for each compound obtained from the thermal graph were utilized to calculate the decomposed species [25].

The following is a summary of the findings:

1. The results and the suggested formulae which are obtained from the analytical data seem to be identical [16].
2. The thermogravimetric analysis data indicates that the process of decomposition for the ligand (TAS) carries out in several steps as well as its complexes.
3. TAS complexes' thermal stability is reduced in the following order:  $[\text{Pt}(\text{TAS})_2] \text{Cl}_2 \cdot 2\text{H}_2\text{O} > [\text{Pd}(\text{TAS})\text{Cl}_2] > [\text{Co}(\text{TAS})_2\text{Cl}_2] > \text{TAS}$

**Table (7): (TGA) of ligand (TAS) and its complexes**

Com. Sym.	Molecular formula(molecular weight) g/mole	Step	TG. Range of the decomposition (°C)	Suggested Assignment	Calculate %	Found %
TAS	$\text{C}_{17}\text{H}_{17}\text{N}_8\text{O}_5\text{S}$ (445.44)	1	(25-350)	$\text{C}_{17}\text{H}_{17}\text{N}_8\text{O}$	78.21	78.43
		2	(350-1000)	$\text{O}_4\text{S}_{0.5}$	18.44	17.95
		Residue	>1000	$\text{S}_{0.5}$	3.32	3.59
$[\text{Pt}(\text{TAS})_2]\text{Cl}_2 \cdot 2\text{H}_2\text{O}$	$\text{Pt} (\text{C}_{34}\text{H}_{38}\text{N}_{16}\text{O}_{12}\text{S}_2) \text{Cl}_2$ (1192.88)	1	(25-90)	$\text{H}_4\text{O}_2$	3.126	3.01
		2	(90-225)	$\text{C}_4\text{H}_7\text{Cl}_2$	10.57	10.56
		3	(225-320)	$\text{C}_5\text{H}_{18}$	6.539	6.51
		4	(320-510)	$\text{C}_8\text{H}_9$	8.788	8.6
		5	(510-1000)	$\text{C}_{17}\text{N}_{16}\text{O}_{10}\text{S}_{1.25}\text{Pt}$	56.83	56.7

				0.25		3
		Residue	>1000	S <sub>0.75</sub> Pt <sub>0.75</sub>	14.15	14.27
[Pd(TAS)Cl <sub>2</sub> ]	Pd(C <sub>17</sub> H <sub>17</sub> N <sub>8</sub> O <sub>5</sub> S)Cl <sub>2</sub> (622.86)	1	(25-370)	C <sub>17</sub> H <sub>17</sub> N <sub>8</sub> O <sub>4.5</sub> Cl <sub>2</sub>	76.43	76.42
		2	(370-1000)	SO <sub>0.5</sub> Pd <sub>0.33</sub>	12.2	12.1
		Residue	>1000	Pd <sub>0.66</sub>	11.36	11.36
[Co(TAS) <sub>2</sub> Cl <sub>2</sub> ] [Ni(TAS) <sub>2</sub> Cl <sub>2</sub> ]	Co(C <sub>34</sub> H <sub>34</sub> N <sub>16</sub> O <sub>10</sub> S <sub>2</sub> )Cl <sub>2</sub> (1020.78)	1	(25-340)	C <sub>8</sub> H <sub>16</sub> Cl <sub>2</sub>	17.93	17.92
		2	(340-510)	C <sub>22</sub> H <sub>10</sub>	26.88	26.84
		3	(510-900)	C <sub>4</sub> H <sub>8</sub> N <sub>16</sub> O <sub>6</sub>	36.5	36.83
		4	(900-1000)	S <sub>0.5</sub> O <sub>4</sub>	8.114	7.83
		Residue	>1000	CoS <sub>1.5</sub>	10.57	10.47

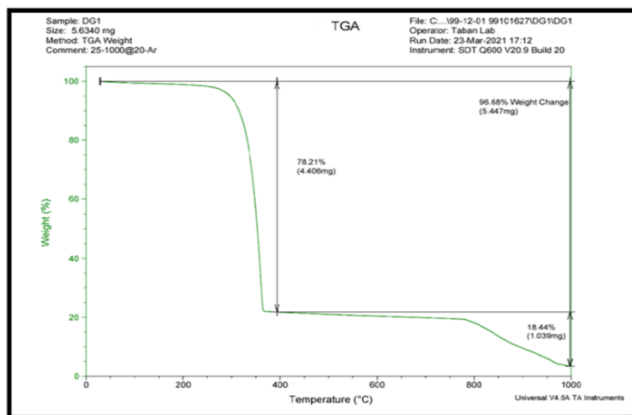


Figure (13): Thermogram of TGA for the TAS ligand

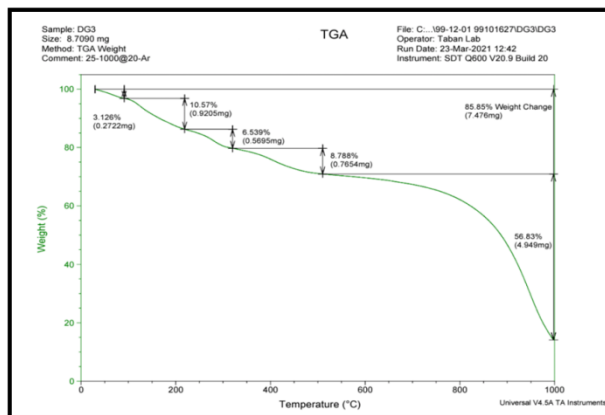


Figure (14): Thermogram of TGA for the [Pt(TAS)<sub>2</sub>]Cl<sub>2</sub>·H<sub>2</sub>O complex

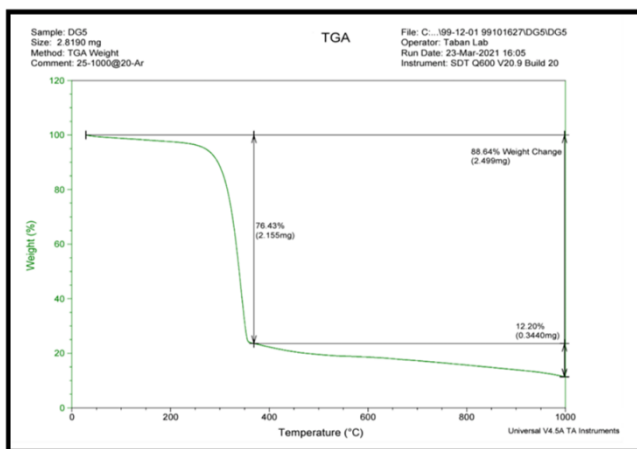


Figure (15): Thermogram of TGA for the [Pd(TAS)Cl<sub>2</sub>] complex

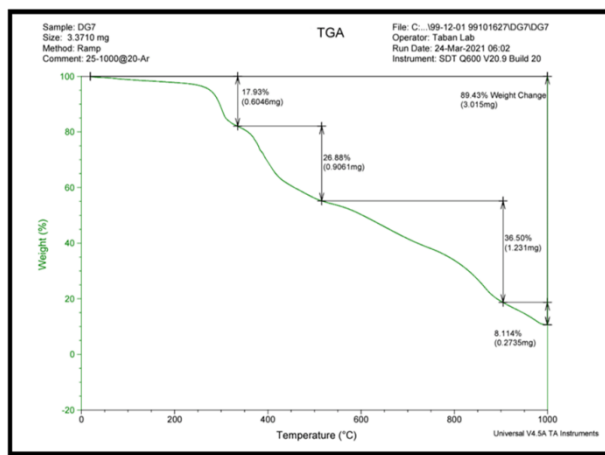


Figure (16): Thermogram of TGA for the [Co(TAS)<sub>2</sub>]Cl<sub>2</sub> complex

### 7-Anti-oxidant and Radical Scavenging Activity

Antioxidants help to stabilize a variety of goods, including meals, petrochemicals, medicines, and cosmetics, as well as also help to strengthen an organism's defenses against free radical assaults. It can be found in both endogenous and exogenous forms in nature [26]. Theobromine can relax the smooth muscle of the trachea and relieve coughs. According to a recent study, it has antioxidant characteristics that are prevalent in pharmacology, demonstrating a positive suppressive effect on oxidative stress [27]. In all concentrations tested (0.08, 0.16, 0.32, and 0.64 mg/ml), [Pd(TAS)Cl<sub>2</sub>] outperformed Trolox (standard) in the concentration-dependent reductive ability. It was (0.6590 ± 0.00529) at 0.08 mg/ml, and increased significantly to (0.7783 ± 0.00472) at 0.64 mg/ml [Table (8)].

**Table (8): Reductive ability of [Pd(TAS)Cl<sub>2</sub>] and Trolox (vitamin E)**

Concentration (mg/ml)	Reductive Ability Absorbance (Mean ± SD)	
	[Pd(TAS)Cl <sub>2</sub> ]	Trolox (Vitamin E)
0.08	0.6590 ± 0.00529	0.108 ± 0.001 <sup>CD</sup>
0.16	0.6763 ± 0.00152	0.114 ± 0.004 <sup>C</sup>
0.32	0.7690 ± 0.00100	0.132 ± 0.007 <sup>B</sup>
0.64	0.7783 ± 0.00472	0.211 ± 0.015 <sup>A</sup>

Antioxidants are chemical compounds that fight and prevent metabolic diseases caused by oxidative stress generated by free radicals when compared to naturally occurring antioxidants, synthetic antioxidants have been demonstrated to have higher antioxidant activity synthetic antioxidants, on the other hand, have a restricted application due to their toxicity. There is a lot of interest in finding a new class of synthetic chemicals that are less toxic and don't have any pathological side effects in this area. As a result, the current research uses the DPPH test. The azo dye ligand (TAS) and its metal complexes were tested for their scavenging activity. Figure (17) shows the scavenging effect of the tested chemicals at various doses, and it's clear that the action is reliant on coordination. Among the substances put to the test when compared to standard, the Pd(II) complex had good scavenging action, ascorbic acid used as control [16]. At the five concentrations examined (12.5, 25, 50, 100, and 200 mg/ml), [Pd(TAS)Cl<sub>2</sub>] was substantially more effective in DPPH radical scavenging activity than vitamin C. At concentrations of 12.5 mg/ml [Pd(TAS)Cl<sub>2</sub>], it was (37.35 ± 0.8214). At 200 mg/ml, DPPH radical scavenging activity increased dramatically to (70.80 ± 2.224). Table (9) shows the results.

**Table (9): DPPH radical scavenging activity of [Pd(TAS)Cl<sub>2</sub>] and vitamin C**

Concentration (mg/ml)	DPPH Radical Scavenging Activity (Mean ± SD; %)	
	[Pd(TAS)Cl <sub>2</sub> ]	Vitamin C
12.5	37.35 ± 0.8214	44.56 ± 1.34
25	40.16 ± 1.974	53.74 ± 2.287
50	56.94 ± 1.621	65.12 ± 5.194
100	65.90 ± 4.922	74.85 ± 1.238
200	70.80 ± 2.224	81.52 ± 3.076

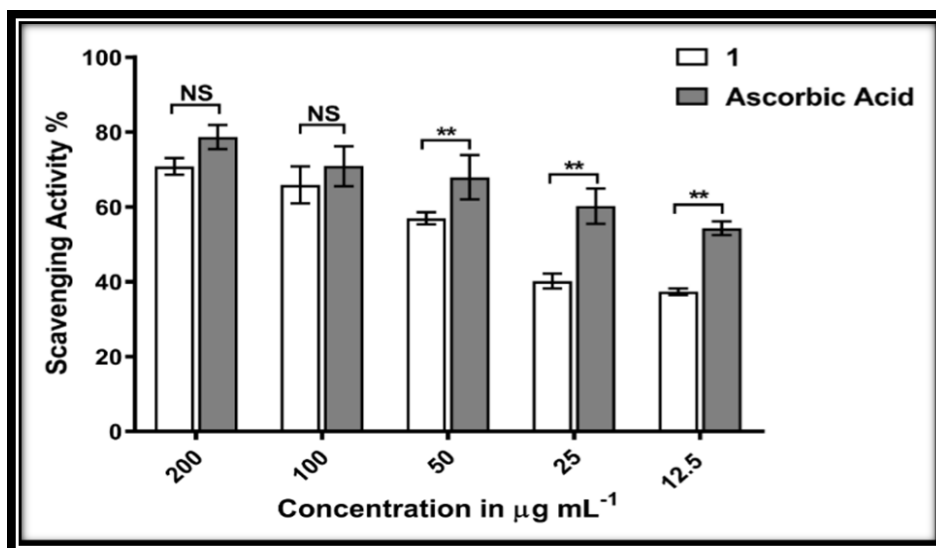


Figure (17): scavenging activity of [Pd(TAS)Cl<sub>2</sub>] complex

### 8- Antibacterial and antifungal Activity

Acertain ligand may react with metal ions in living tissues, inhibiting chelating sites and interfering with normal processes [28].Furthermore, metal ions play an important function in biological systems, whether in metabolism or growth. Metal complexes may be used as medicine to introduce ligands, metal ions, or both to a confirmed site in the living system [21].The numerous pharmacological and chemical features of azo compounds have piqued the interest of many researchers [29]. The antibacterial efficacy of the new azo ligand (TAS) and its complexes were tested in vitro with two pathogenic microorganisms using a disk diffusion technique in (10<sup>-3</sup>M)in ethanol as a solvent, Inhibitory zones (in mm) were measured after the Petri dishes were incubated at 37°C for 24 hours (for bacteria) and 72 hours (for fungi), with sulfamethoxazoleas a control for bacteria and fluconazole for fungi [30]. The pathogenic bacteria used were selected for their ability to produce a wide range of life-threatening illnesses in living systems.There were gram-negative bacteria Escherichia Coli(E.coli) and gram-positive bacteria Staphylococcus aureus (Staph) while the one type of fungi (Rhizopusmicrosporus). The obtained results are provided in Table (10).It was found that most of the testedcompounds had medium to strong activity, except TAS ligand and [Co(TAS)<sub>2</sub>Cl<sub>2</sub>]with (E.coli) bacteria and [Pt(TAS)<sub>2</sub>]Cl<sub>2</sub>.2H<sub>2</sub>O and[Co(TAS)<sub>2</sub>Cl<sub>2</sub>]with (Staph) bacteria, were found they have low activity compared to the sulfamethoxazolewhich served as a reference antibiotic and demonstrated good inhibition of the same harmful bacteria [31]. Metal (II) complexes were shown to be more effective than free ligand, indicating that the reactivity of metal ions with the ligand is significant in increasing antibacterial activity. the lipid membrane that surrounds the cell allows only lipidsoluble molecules to pass through, making

liposolubility an important component in bacterial activity regulation chelation, on the other hand, significantly lowers the polarity of the metal ion due to the partial sharing of its positive charge with the donor groups. Delocalization of the electron on the whole chelating ring enhances the lipophilic character of the central metal atom, which favors its penetration more efficiently through the lipid layer of the cell membrane, thus more aggressively killing them[32]. The presence of metal ions, which are more hypersensitive to microbial cells than the free organic molecule, may account for the increased antibacterial effectiveness following complex formation. Divergence in the activity of various complexes toward different species is caused by variations in ribosomes in microbial cells or the impermeability of microbes' cells [17]. Finally, the ligand and complexes have effectiveness toward *Rhizopus microsporus* fungi, especially  $[Pd(TAS)Cl_2]$  [33].

The activity increases in the following order for (*E.coli*) bacteria :  $[Pt(TAS)_2]Cl_2 \cdot 2H_2O > [Pd(TAS)Cl_2] > [Co(TAS)_2Cl_2] > TAS$

and for (*Staph*) bacteria ,the activity increases in the following order :  $TAS > [Pd(TAS)Cl_2] > [Co(TAS)_2Cl_2] > [Pt(TAS)_2]Cl_2 \cdot 2H_2O$

While the activity for *Rhizopusmicrosporus* fungus increases in the following order :  $[Pd(TAS)Cl_2] > TAS > [Pt(TAS)_2]Cl_2 \cdot 2H_2O > [Co(TAS)_2Cl_2]$

**Table (10): The inhibition zones scale in (mm) of Ethanole, Sulfamethoxazole,fluconazole ,ligand (TAS) and its complexes**

Compounds	Gram Negative	Gram Positive	Rhizopusmicrosporus
	Escherichia coli	Staphylococcus aureus	
ethanole	---	---	---
sulfamethoxazole	36	38	---
fluconazole	---	---	20
TAS	10	17	17
$[Pt(TAS)_2]Cl_2 \cdot 2H_2O$	38	9	16
$[Pd(TAS)Cl_2]$	25	14	23
$[Co(TAS)_2Cl_2]$	11	12	12

### 9-Dyeing performance

The performance of the ligand (TAS) and its complexes as wool dyes were investigated. Wool fiber is made up of protein filaments, the majority of which is keratin, which has a complicated structure with amino groups and carboxyl groups [34]. Early theories of wool dyeing were based on the adsorption of acids by wool. These theories attempted to explain the overall mechanism of wool dyeing under acid conditions solely in terms of the ionic interactions between the positively charged amino groups on the fibers and the negatively charged dye anions [35].

Wool fiber includes a variety of polar groups, including  $-NH$ ,  $-SH$ , and  $-OH$  groups. A terminal amino group, as well as a significant number of  $-NH$  groups, may be found in polyamide fiber. To react covalently with reactive dyes like chlorotriazine and vinylsulphone, each of these functional groups requires a particular pH level. It should be emphasized that in an acid media [36].

The kind of metal and its valence state, the solution concentration, pH, duration, temperature, and other variables all influence the pace and extent of absorption. The free carboxyl groups of acidic amino acids are the most likely binding sites, as they can offer negatively charged binding sites throughout a wide pH range. The nitrogen atoms of amin and amide groups can form coordination bonds, especially at alkaline pH [37]. Figure(18) was shown the wool textile dyeing with the ligand (TAS) and its metal complexes, the colors of wool textile were range between pink and brown.

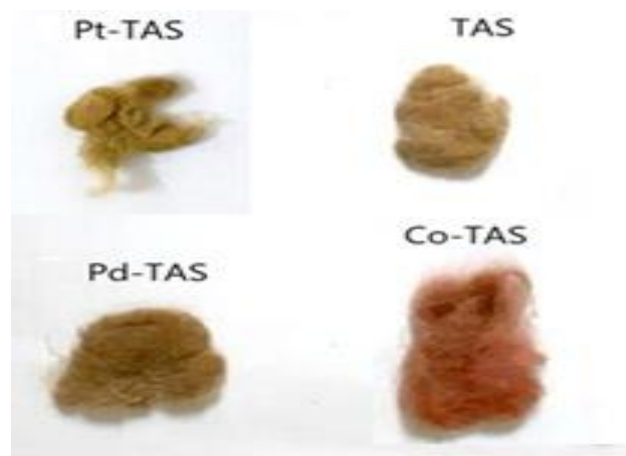


**Figure (18): the wool textile dyeing of ligand (TAS) with its metal complexes**

### Wash Fastness

Textile color fastness test for washing was carried out using soap with a concentration of 2%, and the results were very good. Table (11)



**Table (11): Results of dyeing and various fastness feature of azo ligand (TAS) and its complexes on wool textile**

Number of compounds	Textile color fastness to wet and dry abrasion		Textile color fastness check for washing	
	Dry rubbing	Wet rubbing	Staining with dye	Color change
TAS	5	4/5	2	3/4
(Co-TAS)	4	3	3	4
(Pd-TAS)	5	4	4/5	3
(Pt-TAS)	4	4	1	3

Grading:5-4 (good), 3(moderate), 1-2(not good)

### Conclusion

The ligand (TAS) was synthesized by the diazotization-coupling method, which was acted as neutral N, N-bidentate chelating ligand binds to the metal ions of interest. [Co(II), Pt(II), and Pd(II)] through the nitrogen of azo moiety and (N9) of theobromine that it is formed a pentagonal chelating ring. The octahedral for Co(II) complex but square planar for Pt(II) and Pd(II) complexes. The synthesized complexes were characterized as high stability through examination of the stability constant and not affected by moisture, light, and heat. Also through thermal analysis, the thermal stability of the produced compounds is shown by TGA. The ligand and its complexes have various antibacterial and antifungal activities. Some of the complexes are effective as an antioxidant. The ligand and the complexes can dye wool fabrics as they have different colors.

### References

- [1] Mallikarjuna NM, Keshavayya J. Synthesis, spectroscopic characterization and pharmacological studies on novel sulfamethoxazole based azo dyes. Journal of King Saud University-Science. 2020 Jan 1;32(1):251-259.
- [2] Al-Fregi AA, Al-Salami BK, Al-Khazragie ZK, Al-Rubaie AZ. Synthesis, characterization and antibacterial studies of some new tellurated azo compounds. Phosphorus, Sulfur, and Silicon and the Related Elements. 2019 Feb 1;194(1-2):33-38.
- [3] Gh AB, Khomami SR. Spectrophotometric Study of the Complexation of Sulfa Drugs with Cu (II) and Coupling Reagents in the Presence of Molybdate Ions. Pharmaceutical Chemistry Journal. 2015 May;49(2):132-8.

- [4]Kaur J, Sodhi GS. Diuretic activity of organomercury (II) complexes of theophylline and theobromine. *Journal of inorganic biochemistry*. 1992 Dec 1;48(4):305-10.
- [5]Crowston EH, Goodgame DM, Hayman PB, Slawin AM, Williams DJ. Platinum (II) complexes of methyl-substituted xanthenes: crystal structures of  $K [Pt (theobromine) Cl_3] \cdot H_2O$ ,  $trans-[Pt (isocaffeine) 2Cl_2] \cdot H_2O$  and  $K (isocaffeinium)[PtCl_4] \cdot H_2O$ . *Inorganica Chimica Acta*. 1986 Dec 15;122(2):161-8.
- [6]Abbas AK. Lanthanide Ions Complexes of 2-(4-amino antipyrine)-L-Tryptophane (AAT): Preparation, Identification and Antimicrobial Assay. *Iraqi Journal of Science*. 2015;56(4C):3297-309.
- [7]Fu W, Chen J, Cai Y, Lei Y, Chen L, Pei L, Zhou D, Liang X, Ruan J. Antioxidant, free radical scavenging, anti-inflammatory and hepatoprotective potential of the extract from *Parathelypteris nipponica* (Franch. et Sav.) Ching. *Journal of ethnopharmacology*. 2010 Aug 9;130(3):521-8.
- [8] Sanja SD, Sheth NR, Patel NK, Patel D, Patel B. Characterization and evaluation of antioxidant activity of *Portulacaoleracea*. *Int. J. Pharm. Pharm. Sci*. 2009 Jul;1(1):74-84.
- [9]Abass AK. Synthesis, Structural and Biological Efficiency Studies of New Azo Ligands and Their complexes with Zn (II), Cd (II) and Hg (II) Metal ion. *Ibn AL-Haitham Journal For Pure and Applied Science*. 2017 Mar 14;28(3):169-86.
- [10] Rehab Abd Al-hussein Dabish A. Synthesis and Spectral Studies of Some New Complexes Containing Azo Ligand with Anticancer, Antibacterial and Dyeing Performance. *Annals of the Romanian Society for Cell Biology*. 2021 Apr 21:7968-8006.
- [11] AbouEl-Enein SA, Emam SM, Polis MW, Emara EM. Synthesis and characterization of some metal complexes derived from azo compound of 4, 4'-methylenedianiline and antipyrine: evaluation of their biological activity on some land snail species. *Journal of Molecular Structure*. 2015 Nov 5;1099:567-78.
- [12]Rageh NM. Tautomeric structures, electronic spectra, acid-base properties of some 7-aryl-2, 5-diamino-3 (4-hydroxyphenylazo) pyrazolo [1, 5-a] pyrimidine-6-carbonitriles, and effect of their copper (II) complex solutions on some bacteria and fungi. *Spectrochimica Acta Part A: Molecular and Biomolecular Spectroscopy*. 2004 Jul 1;60(8-9):1917-24.
- [13]Issa YM, El-Hawary WF, Youssef AF, Senosy AR. Spectrophotometric determination of sildenafil citrate in pure form and in pharmaceutical formulation using some chromotropic acid azo dyes. *Spectrochimica Acta Part A: Molecular and Biomolecular Spectroscopy*. 2010 Apr 1;75(4):1297-303.
- [14]Perry DL. *Handbook of inorganic compounds*. CRC press; 2016 Apr 19.

- [15]Birdsall WJ, Taylor DL.Preparation of copper (II) and zinc (II) halide and primary amine complexes of theobromine.Polyhedron. 1989 Jan 1;8(21):2593-7.
- [16]Mallikarjuna NM, Keshavayya J, Maliyappa MR, Ali RS, Venkatesh T. Synthesis, characterization, thermal and biological evaluation of Cu (II), Co (II) and Ni (II) complexes of azo dye ligand containing sulfamethaxazole moiety. Journal of Molecular Structure. 2018 Aug 5;1165:28-36.
- [17]Saad FA, Al-Fahemi JH, El-Ghamry H, Khedr AM, Elghalban MG, El-Metwaly NM. Elaborated spectral, modeling, QSAR, docking, thermal, antimicrobial and anticancer activity studies for new nanosized metal ion complexes derived from sulfamerazineazodye. Journal of Thermal Analysis and Calorimetry. 2018 Feb;131(2):1249-67.
- [18]Karcı F, Demirçalı A, Şener İ, Tilki T. Synthesis of 4-amino-1H-benzo [4, 5] imidazo [1, 2-a] pyrimidin-2-one and its disperse azo dyes. Part 1: Phenylazo derivatives. Dyes and Pigments. 2006 Jan 1;71(2):90-6.
- [19]Bayoumi HA, Alaghaz AM, Aljahdali MS. Cu (II), Ni (II), Co (II) and Cr (III) complexes with N2O2-chelating schiff's base ligand incorporating azo and sulfonamide moieties: spectroscopic, electrochemical behavior and thermal decomposition studies. Int. J. Electrochem. Sci. 2013 Jul 1;8:9399-413.
- [20]Dinçalp H, Toker F, Durucasu İ, Avcıbaşı N, İcli S. New thiophene-based azo ligands containing azomethine group in the main chain for the determination of copper (II) ions. Dyes and Pigments. 2007 Jan 1;75(1):11-24.
- [21]Özerkan D, Ertik O, Kaya B, Kuruca SE, Yanardag R, Ülküseven B. Novel palladium (II) complexes with tetradentatethiosemicarbazones. Synthesis, characterization, in vitro cytotoxicity and xanthine oxidase inhibition.Investigational new drugs. 2019 Dec;37(6):1187-97.
- [22]Mohamed GG, El-Gamel NE, Nour El-Dien FA.Preparation, chemical characterization, and electronic spectra of 6-(2-pyridylazo)-3-acetamidophenol and its metal complexes.Synthesis and Reactivity in Inorganic and Metal-Organic Chemistry. 2001 Feb 28;31(2):347-58.
- [23]Al-Hamdani AA, Hamoodah RG. Transition metal complexes with tridentate ligand: preparation, spectroscopic characterization, thermal analysis and structural studies. Baghdad Science Journal. 2016;13(4).
- [24]Al-Adilee KJ, Abedalrazaq KA, Al-Hamdiny ZM. Synthesis and spectroscopic properties of some transition metal complexes with new azo-dyes derived from thiazole and imidazole. Asian Journal of Chemistry. 2013 Dec 11;25(18):10475.

- [25]Gaber M, El-Wakiel N, Hemeda OM. Cr (III), Mn (II), Co (II), Ni (II) and Cu (II) complexes of 7-((1H-benzo [d] imidazol-2-yl) diazenyl)-5-nitroquinolin-8-ol. synthesis, thermal, spectral, electrical measurements, molecular modeling and biological activity. *Journal of Molecular Structure*. 2019 Mar 15;1180:318-29.
- [26]Ahmad S, Arshad MA, Ijaz S, Khurshid U, Rashid F, Azam R. Review on methods used to determine antioxidant activity. *International Journal of Multidisciplinary Research and Development*. 2014;1(1):35-40.
- [27]Wu F, Liu R, Shen X, Xu H, Sheng L. Study on the interaction and antioxidant activity of theophylline and theobromine with SOD by spectra and calculation. *SpectrochimicaActa Part A: Molecular and Biomolecular Spectroscopy*. 2019 May 15;215:354-62.
- [28]El-Ghamry HA, Fathalla SK, Gaber M. Synthesis, structural characterization and molecular modelling of bidentateazo dye metal complexes: DNA interaction to antimicrobial and anticancer activities. *Applied Organometallic Chemistry*. 2018 Mar;32(3):e4136.
- [29]Ahluwalia VK, Kaur J, Ahuja BS, Sodhi GS. Organomercury (II) complexes of 6-thioguanine: synthesis, characterization, and biological studies. *Journal of inorganic biochemistry*. 1991 May 1;42(2):147-51.
- [30]Schweiger MJ, Beck W. Metal Complexes of Biologically Important Ligands, Part CLXXVIII. Addition of the PentacarbonylrheniumCation  $[(OC)_5Re]^+$  to the Xanthine Alkaloids Caffeine, Theophylline, and Theobromine. *Zeitschriftfüranorganische und allgemeineChemie*. 2017 Nov 17;643(21):1335-7.
- [31]Jain R, Singh R, Kaushik NK. Synthesis, characterization, and thermal and antimicrobial activities of some novel organotin (IV): Purine base complexes. *Journal of Chemistry*. 2013 Jan 1;2013.
- [32]Bouhdada M, Amame ME, El Hamzaoui N. Synthesis, spectroscopic studies, X-ray powder diffraction data and antibacterial activity of mixed transition metal complexes with sulfonateazo dye, sulfamate and caffeine ligands. *Inorganic Chemistry Communications*. 2019 Mar 1;101:32-9.
- [33]Habiba I, Saoudi M, Berrah F, Benmerad B, Boudraa M, Merazig H, Bouacida S. A new complex of Zinc (II) with sulfamethoxazole ligand: Synthesis, crystal structure, Hirshfeld surface analysis, thermal properties, DFT calculations and antibacterial/antifungal activities. *Journal of Molecular Structure*. 2021 Jun 16:130903.
- [34]Flath HJ. Textile Dyeing, 3. Dyeing of Wool and Silk. *Ullmann's Encyclopedia of Industrial Chemistry*. 2000 Jun 15:1-9.

[35]Lewis DM, Rippon JA, editors. The coloration of wool and other keratin fibres. John Wiley & Sons; 2013 May 20.

[36]Marie MM, Salem AA, El Zairy EM. A novel printing method to enhance the fixation of reactive dyes on wool–polyamide fabrics. Journal of the Textile Institute. 2011 Sep 1;102(9):790-800.

[37]Ferrero F, Periolatto M. Ultrasound for low temperature dyeing of wool with acid dye. Ultrasonics Sonochemistry. 2012 May 1;19(3):601-6.